JOURNAL OF GEOPHYSICAL RESEARCH, VOL. 86, NO. B11, PAGES 10242–10256, NOVEMBER 10, 1981

The Mineralogy and Chemistry of the Anorogenic Tertiary Silicic Volcanics of S.E. Queensland and N.E. New South Wales, Australia

A. EWART

Department of Geology & Mineralogy, University of Queensland, St. Lucia, Brisbane, Queensland 4067

The Late Oligocene-Early Miocene volcanism of this region is chemically strongly bimodal; the mafic lavas (volumetrically dominant) comprise basalts, hawaiites, and tholeiitic andesites, while the silicic eruptives are mainly comendites, potassic trachytes, and potassic, high-silica rhyolites. The comendites and rhyolites have distinctive trace element abundance patterns, notably the extreme depletions of Sr, Ba, Mg, Mn, P, Cr, V, and Eu, and the variable enrichment of such elements as Rb, Zr, Pb, Nb, Zn, U, and Th. The trachytes exhibit these characteristics to lesser degrees. The comendites are distinguished from the rhyolites by their overall relative enrichment of the more highly charged cations (e.g., LREE, Nb, Y, and especially Zr) and Zn. The phenocryst mineralogy of the trachytes and rhyolites comprises various combinations of the following phases: sodic plagioclase (albite-andesine), calcic anorthoclase, sanidine, quartz, ferroaugite-ferrohedenbergite, ferrohypersthene, fayalitic olivine, ilmenite, titanomagnetite, and rarely biotite (near annite) and Fe-hastingsitic amphibole. Accessories include apatite, zircon, chevkinite (ferrohedenbergite-bearing rhyolites only), and allanite (amphibole and botite rhyolites only). The comendites generally contain Ca-poor anorthoclase-sanidine, quartz, fluorarfvedsonite, aegirine and aegirine-augite (Zr-bearing), aenigmatite, and ± ilmenite. Coexisting Fe-Ti oxides are absent in the comendites and relatively uncommon in the rhyolites and trachytes. Where present, they indicate equilibration temperatures of 885°–980°C and fo_2 between QFM and WM buffers. The magmas are thus interpreted to have been strongly water undersaturated during phenocryst equilibration, which is also consistent with the general paucity of pyroclastics, the rarity of hydrous mineral phases, and the extreme Fe-enriched ferromagnesian phenocryst compositions. The chemical and mineralogical data are interpreted to indicate the operation of extreme fractionation processes controlling the development of the silicic magmas, and the comendites, trachytes, and certain trachyte-rhyolite series are considered to have evolved from a mafic parentage. The available oxygen, Sr, and Pb isotopic data, however, point to some modification of the magnas through crustal equilibration processes. The remaining high-silica rhyolites are considered to most likely represent crustal partial melts but are again modified by extensive fractionation.

INTRODUCTION

The region in question forms part of the broad belt of Cainozoic volcanism, some 3000 km long, that extends along the eastern and southeastern coastal region of Australia. *Wellman and McDougall* [1974] have shown that volcanic activity commenced about 70 Ma ago and has continued through the Cainozoic at a nearly constant rate. More than 50 volcanic provinces are recognized throughout the whole coastal region. Although basalts, hawaiites and tholeiitic andesites are the dominant lavas, some of the provinces contain minor associated silicic volcanism, namely trachytes, rhyolites, and/or comendites. In certain areas, especially southern Queensland, isolated outcrops of trachytes and comendites are found with apparently no associated mafic extrusives.

Consideration of the overall distribution of chemistry of the erupted magmas in S.E. Queensland reveals that the volcanism is very strongly bimodal [*Ewart et al.*, 1980]. Where both mafic and silicic eruptives occur within a given center, estimates suggest that the relative volumes are at least 7:1 in favor of the mafic eruptives.

The following is a brief outline of the volcanism found within some of the more prominent volcanic centers to which particular references are made in this paper and which indicate the diversity found among the various provinces. A locality map, showing the extent of the S.E. Queensland-N.E. New South Wales volcanic regions, is provided in Figure 1.

Tweed Shield Volcano. This constitutes the eroded remnants of a former shield volcano some 100 km in diameter. The generalized volcanic succession comprises a lower mafic sequence followed by several distinct rhyolite units (two of which are considered in this paper, namely the Binna Burra and Springbrook rhyolites) that are overlain by a younger mafic sequence; a separate comenditic dyke phase also occurs. Volcanism is dated from 20.5–22.3 Ma [*Ewart et al.*, 1977].

Focal Peak Shield Volcano. This again constitutes the eroded remnants of a shield volcano situated within a complex ring structure some 14 km in diameter, the periphery of which is marked by rhyolite intrusions and extrusions (the Mt. Gillies Rhyolites). The massive Mt. Barney granophyre plug also outcrops within this ring structure. The generalized volcanic succession comprises an older mafic sequence followed by the Mt. Gillies Rhyolites. Reported ages range between 23 and 25.6 Ma [*Ross*, 1977].

Glass Houses and Maleny Centers. The Glass House Mountains constitute a spectacular group of eroded domes and plugs composed mainly of comendites but with subordinate trachytes. A few kilometers to the north of these plugs is the isolated mafic Maleny eruptive center, which may be related to the Glass House extrusions. This is supported by K-Ar dates of 25.2 and 25.4 Ma for a young Maleny flow and a comendite, respectively. Extending NNE along the S.E. Queensland coast are several quite isolated silicic extrusive centers, namely, the Mt. Coolum comendite and the Fraser Island trachytes.

Mt. Alford Ring Complex. This represents an eroded plug of microdiorite and subordinate granophyre intruded by a core of tholeiitic andesite; the complex is cut by a semicircular zone of rhyolitic and trachytic ring dykes (25.2 Ma) and a second nonarcuate set of cross-cutting rhyolite, comendite, and basalt dykes [*Stevens*, 1962].

Paper number 1B0531.
0148-0227/81/001B-0531$01.00

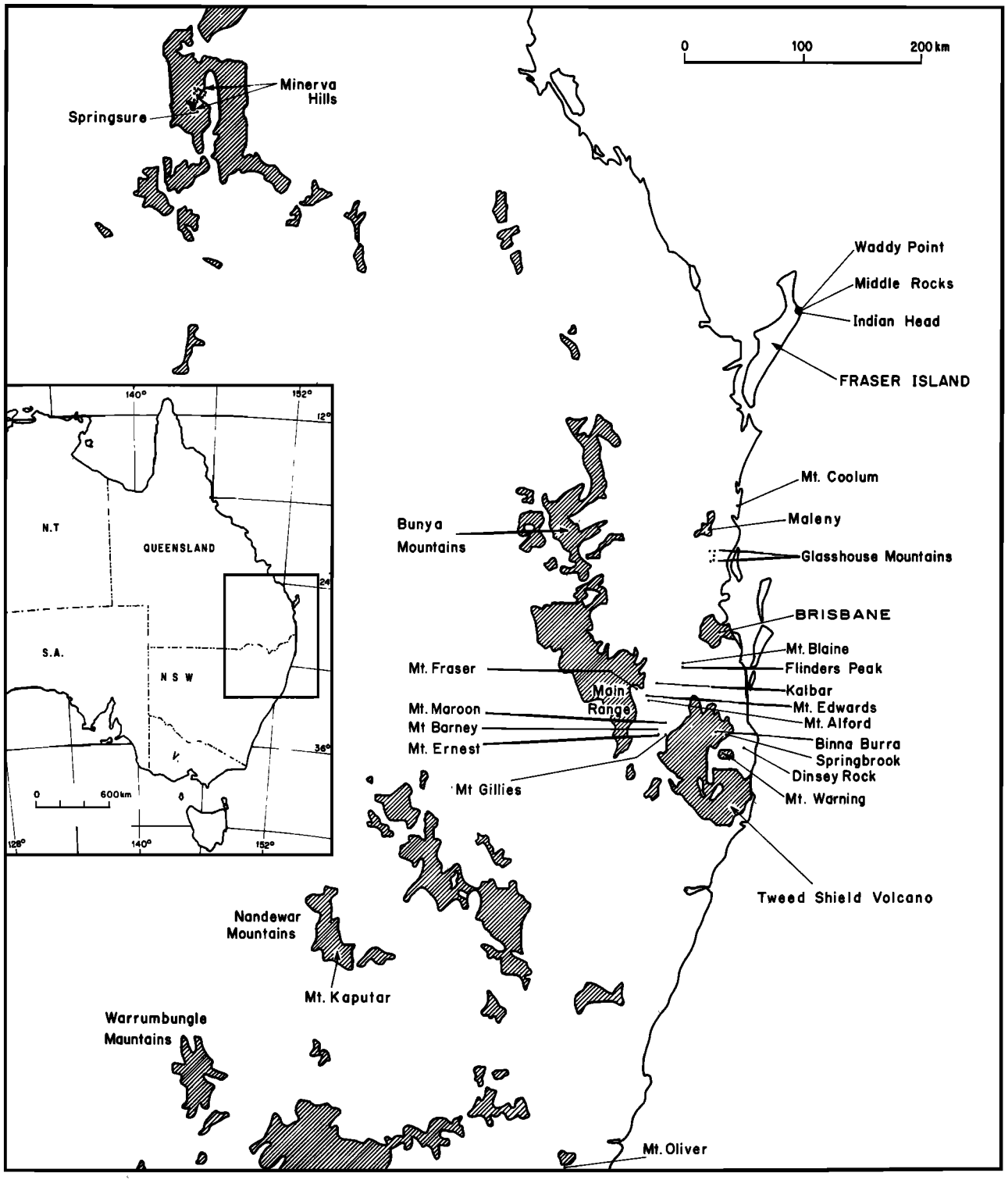

Fig. 1. Map of S.E. Queensland and N.E. New South Wales showing the distribution of the Tertiary volcanic centers.

Minerva Hills. The volcanic sequence from this rather complex center has been broadly divided into a basal series of mafic lavas (some 70 m thick) that are overlain by a younger series of intercalated mafic lavas and trachytic pyroclastics. K-Ar dates of approximately 33–34 Ma and 24–28.5 Ma are obtained from the two series, respectively. The pyroclastics are closely associated with a concentration of numerous plugs, domes, thick flows, sills, and dykes of mainly trachyte with subordinate rhyolite. These are the Minerva Hills volcanics [*Veevers et al.*, 1964].

CHEMISTRY

It is emphasized that within the volcanic provinces being considered there is a strong bimodality of magma compositions with respect to their SiO_2 distributions [*Ewart et al.*, 1980]. This paper is concerned with the silicic compositions,

i.e., those that are greater than 59% SiO_2. In addition, some mineralogical comparisons are made with associated, although rare, microsyenites that occur in certain of the volcanic centers. Averaged major and trace element data and mineralogical data, are summarized in Table 1. The trachyte data are based on sequential averages with increasing SiO_2 contents of the respective samples.

For purposes of this paper the distinction between trachytes and rhyolites is taken as 73% SiO_2. The peralkaline types are readily distinguished by their distinctive sodic mineralogy. Very rare lavas occur that are described as dacites; these are readily distinguished from trachytes by the absence of both phenocrystal alkali feldspar and quartz. In this paper, four distinct types of rhyolites are recognized on the basis of both occurrence and mineralogical criteria (Table 1).

Major Elements

A. Metaluminous and peraluminous rhyolites and trachytes. The majority of the trachytes and rhyolites analyzed are chemically very close to the metaluminous/peraluminous boundary, and it is believed that the magmas were metaluminous prior to the processes of cooling and devitrification. No evidence, however, of the occurrence of systematic selective alkali leaching within the various extrusives has been found. The silicic extrusives of Minerva Hills and the hypersthene-bearing rhyolites are noteworthy in that they consistently show peraluminous chemistry.

The trachytes and rhyolites are all relatively potassic and exhibit progressively depleted Ti, Fe, Mg, Mn, Ca, and P abundances with increasing SiO_2, culminating in very strong depletions of these elements in the rhyolites (the hypersthene rhyolites exhibiting least depletion). Figure 2 indicates that the normative compositions of the rhyolites (excepting the Minerva type) closely approach the quartz-saturated two-feldspar boundary curve (Figure 2*a*) and the 'minimum' (piercing point) in the projection of the $[Ab\text{-}Or\text{-}Q]_{97}An_3$ system (Figure 2*b*) [*James and Hamilton,* 1969], although plotting within the sanidine fields. These can be classed as high-silica, potassic rhyolites. The plots of the trachytes within the quartz-feldspar system (Figure 2*b*) show that they lie in a zone close to, and essentially parallel to, the projection of the two-feldspar boundary curve as defined by *James and Hamilton* [1969] for those compositions low in normative An (see also Figure 2*a*). The Minerva Hills extrusives seem to be unique within the region in that they show a complete continuity of major element chemistry from trachyte to rhyolite in the one volcanic center; it is thus noteworthy that the Minerva rhyolites are lower in normative *Q* (Figure 2*b*) and generally exhibit a more trachytic chemistry compared to the other rhyolites of the region (Table 1).

B. Peralkaline extrusives. These are characterized by normative ac, and less commonly normative ns. The majority of the extrusives are highly silicic and can be classified as comendites (Table 1), although peralkaline trachytes sporadically occur. The comendites exhibit highly depleted Mg, Mn, Ca, and P abundances, with Na and Fe^{3+} significantly enriched compared to the nonperalkaline rhyolites. Their normative compositions, when plotted in the quartz-feldspar system (Figure 2*b*), project in a zone lying between the thermal valley in the ternary system [*Tuttle and Bowen,* 1958] and the projection of the two-feldspar boundary curve in the $[Ab\text{-}Or\text{-}Q]_{97}An_3$ system; a systematic shift of Ab/Or ratios therefore occurs with increasing normative *Q*.

Trace Elements

Three distinct patterns of trace element behavior are recognizable within the silicic eruptives of this province:

1. Those behaving as incompatible elements, which thus show a progressive and regular enrichment through the trachyte to rhyolite compositional spectrum: Rb, Th, and to a lesser extent Pb are the most notable examples in this province. For example, there is an almost logarithmic relationship between Rb versus K/Rb [*Ewart et al.,* 1976], which suggests that Rb is effectively excluded from fractionating phenocryst phases (except biotite, which is, however, a very rare phase in the extrusives of the region). This is confirmed by analyses of phenocryst phases from the silicic eruptives. Thus, measured Rb partition coefficients for alkali feldspars range between 0.31 and 0.65 (averaging 0.46) and are <0.1 for all other phases (except biotite). Th partition coefficients are also low, except for certain accessories (zircon, allanite, and chevkinite), while Pb partition coefficients are uniformly higher for the feldspars (0.5 to 1.7).

2. Those elements exhibiting very strong depletion through the compositional spectrum from trachyte to rhyolite, most notably Ba, Sr, V, Ni, and Cr, and also including Mg, Mn, Ca, and P. Extreme Eu depletion also occurs [*Ewart et al.,* 1976]. Such depletions are illustrated by the plot of Rb versus Ba (Figure 3). The behavior of these elements can, in principle, be explained by fractionation of feldspars and Fe-Mg silicates.

3. The highly charged cations, notably Zr, Ce, Y, and Nb. Although these elements normally exhibit enrichment during crystal fractionation within the S.E. Queensland silicic magmas, they also exhibit a mutally 'decoupled' behavior, resulting in poor correlations (Figure 4). This behavior can probably be attributed mainly to the crystallization and fractionation of minor microphenocryst phases such as zircon, chevkinite, allanite, and possibly apatite, in the nonperalkaline lavas, and to sodic pyroxenes and sodic amphiboles in the peralkaline types.

The averaged data for the rhyolites (presented in Table 1) illustrates the above patterns of behavior, and their overall element abundance patterns would seem to be readily interpreted as indicating strong crystal fractionation control (see, however, *Hildreth* [1979] and later discussion). Nevertheless, it is apparent that each rhyolite type has its own distinctive trace element patterns, indicating an independent line of evolution. The Minerva Hills trachytes and rhyolites exhibit a complete continuity of trace element abundances, in conformity with their major element chemistry, and the rhyolites are notably enriched in Zr and Nb compared to the other rhyolite types within the region.

The comendites have certain trace element characteristics (Table 1) that tend to distinguish them from the nonperalkaline rhyolites, most notably the strong enrichments of the highly charged cations (e.g., Zr, Nb, LREE, Y) and Zn. Nevertheless, Table 1 and Figure 4 show that the nonperalkaline trachytes and rhyolites may also exhibit enriched concentrations of certain of these elements, overlapping the abundances found in the comendites. The factor that seems to most characterize the comendites is the relative enrichment of the whole spectrum of the highly charged cations, which is not found in the nonperalkaline lavas. The enrichment of Zr in the comendites is particularly characteristic [see also *Nicholls and Carmichael,* 1969] and is readily explicable by the experi-

TABLE 1. Averaged Major Element, Trace Element, and Mineralogical Data for the S.E. Queensland Trachytes (Based on Sequential Averages), Rhyolites, and Comendites

	Trachytes†			Minerva Hills Trachytes		Rhyolites, >73%				
SiO_2 Range	<66%	66%–69%	69%–73%	66%–69	69%–73%	Hypersthene-Bearing Type	Ferrohedenbergite-Fayalite Type	Binna Burra Type	Minerva Hills Type	Average Comendite >69%
SiO_2	63.15	67.92	69.79	67.79	71.19	76.57	76.02	76.72	73.80	74.28
TiO_2	0.49	0.50	0.45	0.25	0.16	0.26	0.17	0.07	0.14	0.21
Al_2O_3	16.57	15.25	15.67	16.33	15.75	12.23	12.30	12.57	15.06	12.17
Fe_2O_3	2.97	2.41	1.17	3.95	1.54	0.68	0.72	0.77	0.90	2.37
FeO	3.15	1.88	1.45	0.03	0.25	0.94	1.16	0.46	0.04	0.97
MnO	0.13	0.09	0.04	0.08	0.03	0.02	0.03	0.01	0.004	0.04
MgO	0.42	0.24	0.41	0.08	0.06	0.18	0.15	0.03	0.05	0.04
CaO	1.95	1.21	1.05	0.58	0.43	0.60	0.68	0.44	0.21	0.13
Na_2O	5.61	5.03	4.66	5.11	4.90	3.27	3.42	3.60	4.79	5.10
K_2O	5.41	5.37	5.21	5.75	5.65	5.20	5.32	5.31	4.99	4.67
P_2O_5	0.15	0.10	0.10	0.05	0.02	0.05	0.02	0.01	0.02	0.01
Trace Elements, ppm										
Rb	104	115	134	128	165	228	165	471	173	258
Ba	788	835	869	226	64	206	96	11	30	22
Sr	112	80	164	27	12	41	11	1	6	2
Pb	14	15	16	13	14	20	22	44	15	30
Zn	129	169	137	161	174	51	145	147	114	240
Zr	742	724	549	966	612	195	387	137	562	1228
Th	9	10	12	17	22	20	20	44	20	33
Nb	68	53	45	144	198	12	35	58	188	147
Ce	124	155	114	280	156	76	168	60	99	141
Y	50	61	56	79	86	34	74	95	77	120
Cr	0.5	1	1	0.5	1	2	1	<0.5	0.5	<0.5
V	0.5	2	2	<0.5	<0.5	4	2	1	<0.5	1
Phenocryst Mineralogy, modal, vol %										
Plagioclase	—	1.8	3.8	—	0.1	2.8	—	0.2	<0.1	—
Alkali feldspar	8.8	10.7	9.7	5.1	4.3	2.1	11.9	1.2	6.8	3.4
Quartz	—	—	3.3	—	0.3	0.6	3.5	0.7	—	0.5
Clinopyroxene	0.5	0.7	0.2	0.3	0.1	—	0.7	—	<0.1	0.06
Orthopyroxene	—	—	—	—	—	0.6	—	—	—	—
Olivine	0.3	0.4	0.1	0.1	<0.1	—	0.2	—	<0.1	—
Amphibole	—	—	—	—	<0.1	—	—	—	<0.1	0.1
Biotite	—	—	0.1	—	—	—	—	<0.1	—	—
Fe-Ti oxides	0.3	0.2	0.1	0.2	0.1	0.1	0.1	0.1	0.1	0.04
Total phenocrysts	9.9	13.8	17.3	5.7	4.9	6.2	16.4	2.2	6.9	4.1
n*	6	9	5	3	19	3	18	10	8	14

Major elements recalculated on anhydrous basis.
* Number of samples within each data grouping.
† Excluding Minerva Hills.

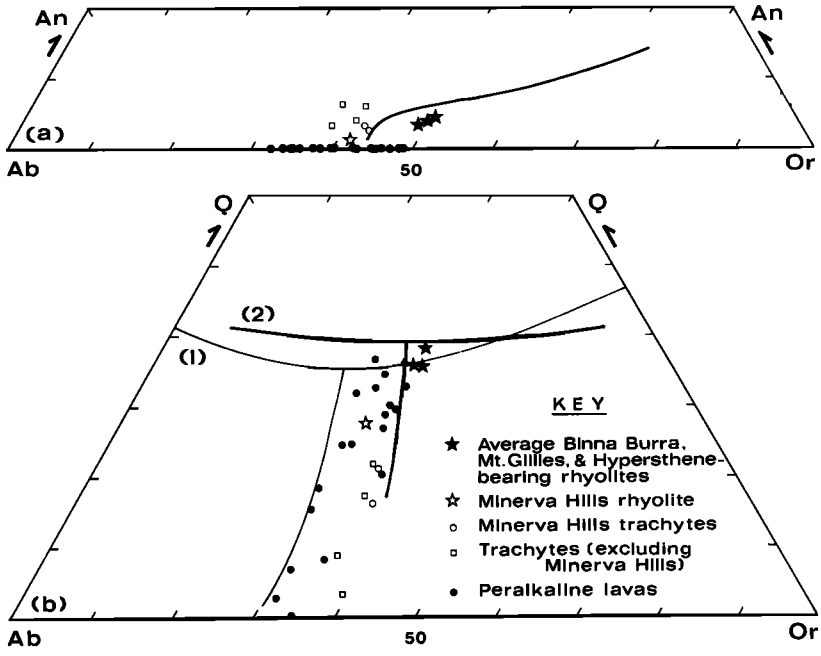

Fig. 2. Normative (CIPW) quartz and feldspar compositions of trachytes, rhyolites, and peralkaline lavas plotted in the quartz-feldspar and feldspar ternary systems. Heavy solid curve in plot (*a*) represents quartz-saturated two-feldspar boundary curve, and in plot (*b*) (curve 2) represents the quartz-feldspar and two-feldspar boundary curves for composition $(Ab\text{-}Or\text{-}Q)_{97}An_3$ (at 1-kbar water vapor pressure), both after *James and Hamilton* [1969]. Curve labeled (1) in plot (*b*) is after *Tuttle and Bowen* [1958] (also for 1 kbar).

mental work of *Watson* [1979], which shows that zircon crystallization is inhibited in peralkaline liquids, supporting the petrographic observations of the absence of zircon in the comendites. This may also explain the enrichment of Y and Th in these peralkaline magmas.

The comendites also exhibit enrichments of Rb and Pb (and probably also such elements as Ga, Be, and U, for which only limited data are available; see *Ewart et al.* [1976]). In contrast, extreme depletions are observed for Ba, Sr, Eu, Ni, Cr, V, Mg, Mn, Ca, and P.

MINERALOGY

Introduction

The following characteristic phenocryst assemblages are observed:

Rhyolites. (a) Sodic plagioclase + sanidine + quartz + Fe-biotite + allanite ± ilmenite ± titanomagnetite. (b) Sanidine + quartz + fayalite + ferrohedenbergite + chevkinite + ilmenite ± titanomagnetite. (c) Sodic plagioclase + quartz + sanidine + ferrohypersthene + ilmenite.

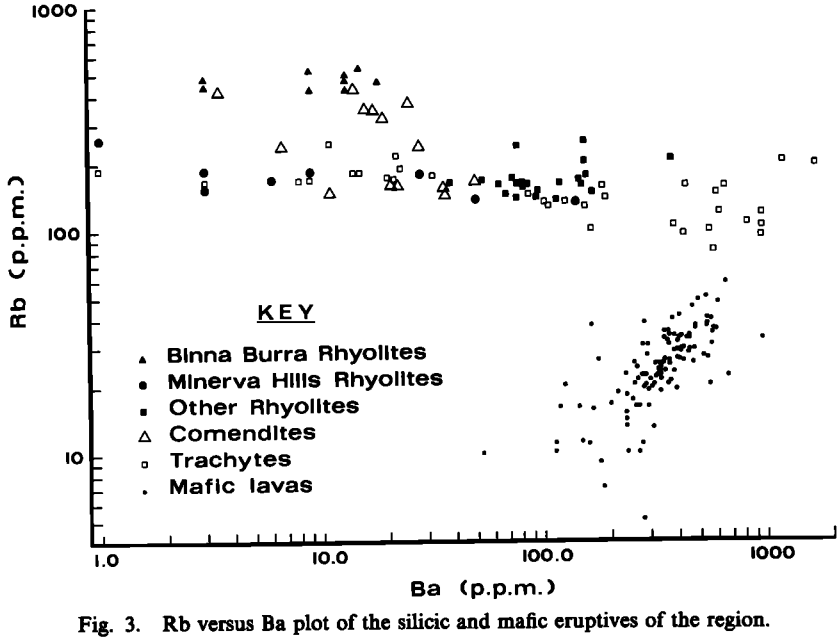

Fig. 3. Rb versus Ba plot of the silicic and mafic eruptives of the region.

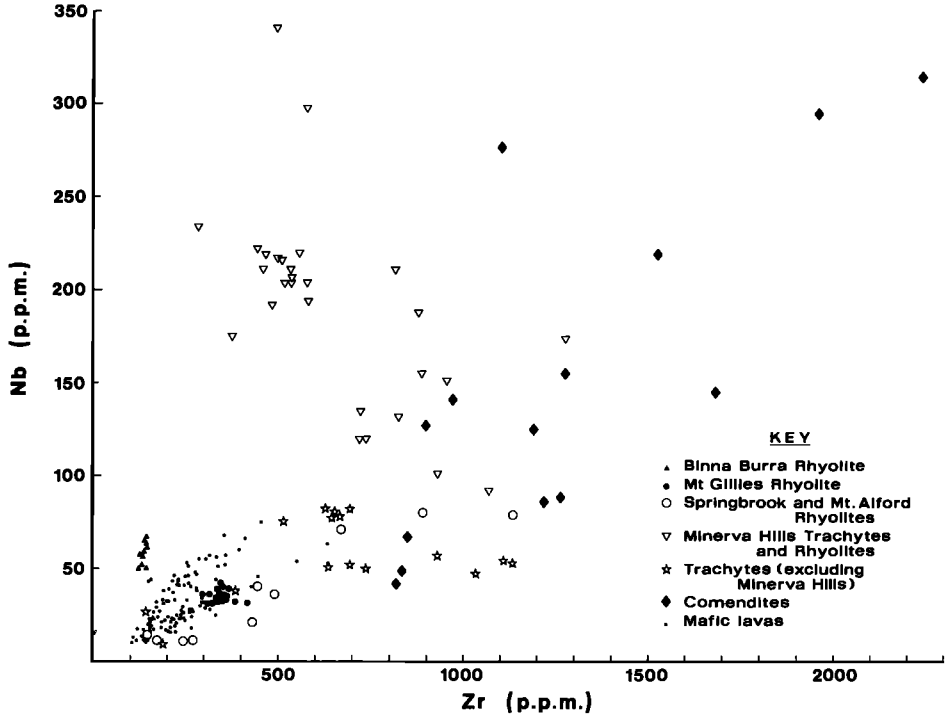

Fig. 4. Zr versus Nb plot of the silicic and mafic eruptives of the region.

Nonperalkaline trachytes. (a) Sanidine + sodic plagioclase + Fe-olivine + ferroaugite + titanomagnetite ± ilmenite. (b) Sanidine-anorthoclase + ferroaugite ± Fe-olivine + titanomagnetite ± ilmenite. (c) Sanidine + hastingsitic amphibole + allanite + ilmenite + titanomagnetitie ± fayalite ± ferrohedenbergite.

Dacites. Plagioclase + augite + ferropigeonite + ilmenite.

Comendites. (a) Phenocrysts: Ca-poor anorthoclase-sanidine ± quartz ± ferrohedenbergite (zoned to aegirine-augite) ± ilmenite. (b) Groundmass: Ca-poor anorthoclase-sanidine + quartz ± aegirine + fluorarfvedsonite ± aenigmatite ± ilmenite.

The silicic magmas from this province were erupted with relatively low phenocryst contents (<10%), although some variation is found, as illustrated in Figure 5 (see also Table 1). No systematic overall differences are apparent between the trachytes, rhyolites, and comendites in their volume percent phenocrysts.

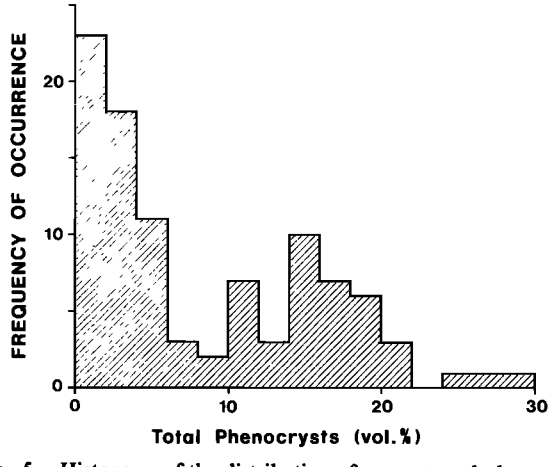

Fig. 5. Histogram of the distribution of percent total phenocrysts in the silicic eruptives (including peralkaline and nonperalkaline types).

Feldspar Phenocrysts

A. Nonperalkaline eruptives. Individual specimens may contain coexisting plagioclase + sanidine, calcic anorthoclase + sanidine, sanidine, calcic anorthoclase zoned to sanidine, or rarely, plagioclase + anorthoclase + sanidine. Compositional relations are thus complex. Extensive chemical zoning occurs in both plagioclase and the alkali feldspars, usually amounting to at least 20 mol. %; the plagioclases and sanidines are zoned to more sodic rims, while the calcic anorthoclase phenocrysts are commonly zoned toward sanidine rims (varying from Or_{25-50}). In certain of the lavas, cores of sodic plagioclase are enclosed by sharply defined zones of sanidine.

Composite plots of the feldspar compositions (microprobe analyses) occurring within the microsyenites, trachytes, and rhyolites are presented in Figure 6. The trachytic feldspar phenocrysts exhibit extensive ternary solid solution, which decreases somewhat in the most siliceous trachytes. Calcic anorthoclase is characteristic of the less siliceous trachytes, whereas the more siliceous trachytes contain a much wider spectrum of compositions, which extend from andesine through to sanidine (Or_{65}). The rhyolitic feldspars are equally variable. The Minerva Hill type is dominated by anorthoclase-sanidine, with rare occurrences of a primary but unusually sodic plagioclase (averaging $An_{6.5}Or_{8.7}$). The Mt. Gillies rhyolites contain almost exclusively sanidine, which occasionally contains cores of corroded plagioclase. The Binna Burra and the hypersthene rhyolites contain coexisting plagioclase and sanidine, the latter rhyolite type having generally more calcic plagioclases.

B. Peralkaline eruptives. Composite plots of the feldspars (Figure 7) in these magmas reveal that Ca-poor anorthoclase-sanidine is the only type found, although considerable compo-

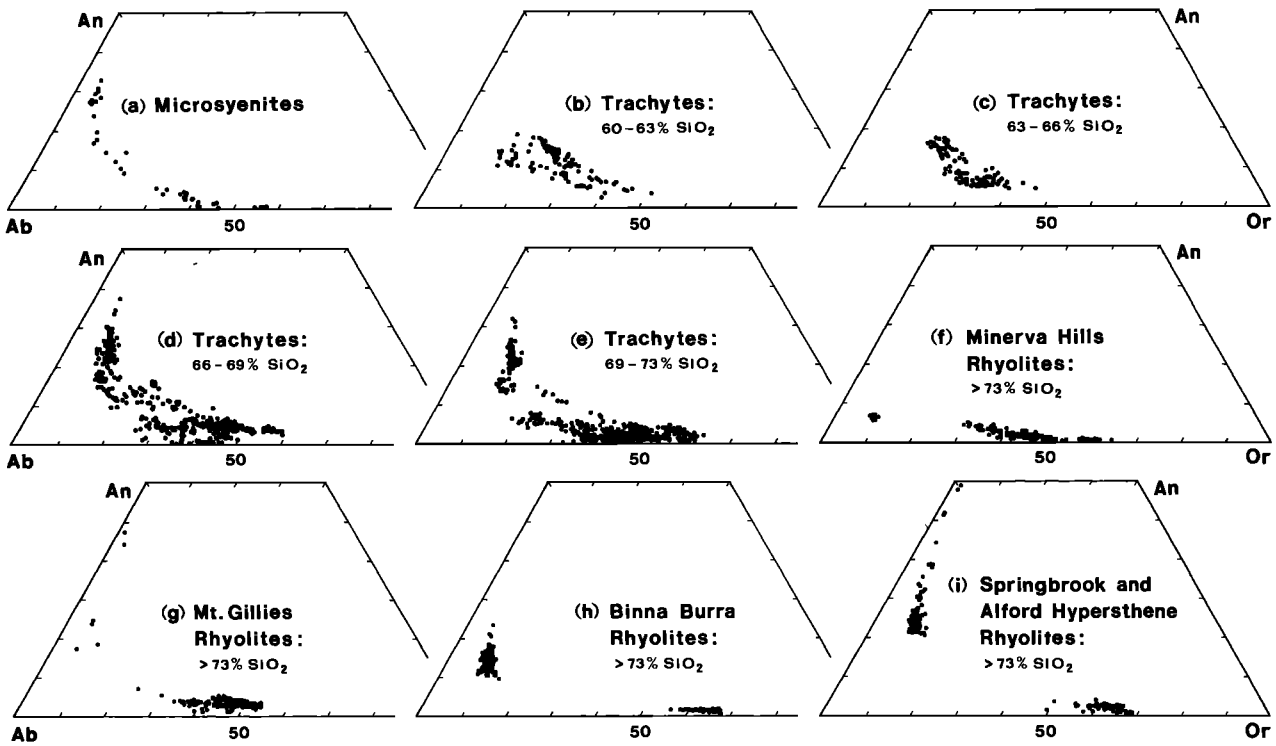

Fig. 6. Composite plots of phenocryst feldspar compositions (mol. %), based on microprobe data, occurring within the microsyenites, trachytes (sequentially subdivided according to total rock silica contents), and rhyolite types.

sitional variation is apparent, that can be broadly correlated with the whole rock normative Ab/Or ratios (Figure 2*b*). Thus the feldspars in the siliceous comendites tend to be more potassic (Or_{37-45}) than those occurring in the less siliceous peralkaline magmas (Or_{22-45}).

Pyroxenes and Olivines

Four distinct pyroxene occurrences are recognized, as follows: (a) phenocrysts of ferroaugite-ferrohedenbergite (± fayalitic olivine); (b) phenocryst ferrohypersthene; (c) phenocryst ferropigeonite (± ferrohypersthene); and (d) ferrohedenbergite-aegirine solid solution series occurring as groundmass phases within the peralkaline extrusives.

In addition, magnesian orthopyroxene, augite, and olivine phases are found in a dacite flow (hybrid), and very rarely in the hypersthene rhyolites, and are clearly xenocrystal.

Figure 8 illustrates the pyroxene compositions found within the trachytes, the pyroxene-bearing rhyolites, and a hybrid dacite. It is clear that these anorogenic silicic magmas are characterized by the development of extreme Fe-enrichment in their phenocryst pyroxenes and olivines, with ferroaugite-ferrohedenbergite being the dominant pyroxene in the nonperalkaline magmas (Table 2). Ferrohypersthene (extending to Fs_{75}) occurs as the characteristic ferromagnesian phenocryst phase in the Springbrook rhyolite and also within isolated rhyolites from the Mt. Alford and Mt. Gillies groups (Table 3). Ferropigeonite occurs as a distinctive phenocryst phase in a unique hybrid dacite flow and very rarely in samples of the Mt. Gillies ferrohedenbergite-fayalite rhyolites. The conditions of precipitation of ferropigeonite are unknown, as it does not occur with coexisting Fe-Ti oxides in these Queensland lavas.

Na-enrichment in the pyroxenes. The extent of Na-enrichment in the pyroxenes from the peralkaline magmas, nonperalkaline magmas, and intrusive microsyenites is compared in Figure 9. It is clear that Na-enrichment is relatively minor in the nonperalkaline magmas, whereas the peralkaline magmas are characterized by complete solid solutions between pure aegirine and ferrohedenbergite, nearly always as groundmass phases. It is therefore evident that Na-enrichment in these pyroxenes occurs only after extreme Fe-enrichment has been attained. A notable feature of the chemistry of the sodic pyroxenes is their relatively high ZrO_2 (Table 4), which is, however, very variable even within the one sample.

Possible factors leading to Na-enrichment in pyroxenes during fractional crystallization can be approached by considering the following two exchange reactions:

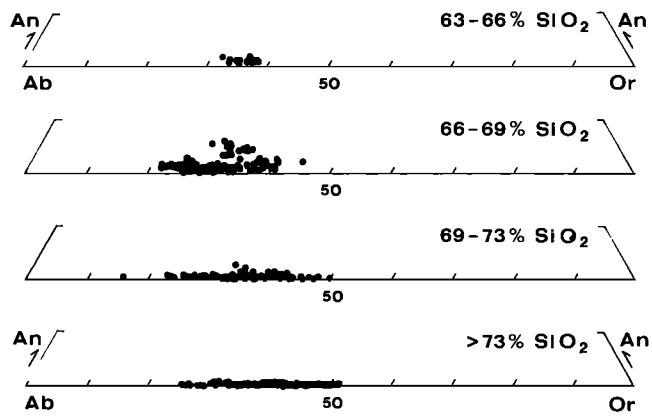

Fig. 7. Composite plots of phenocryst feldspar compositions (mol. %), based on microprobe data, occurring within the peralkaline extrusives (subdivided according to total rock silica contents).

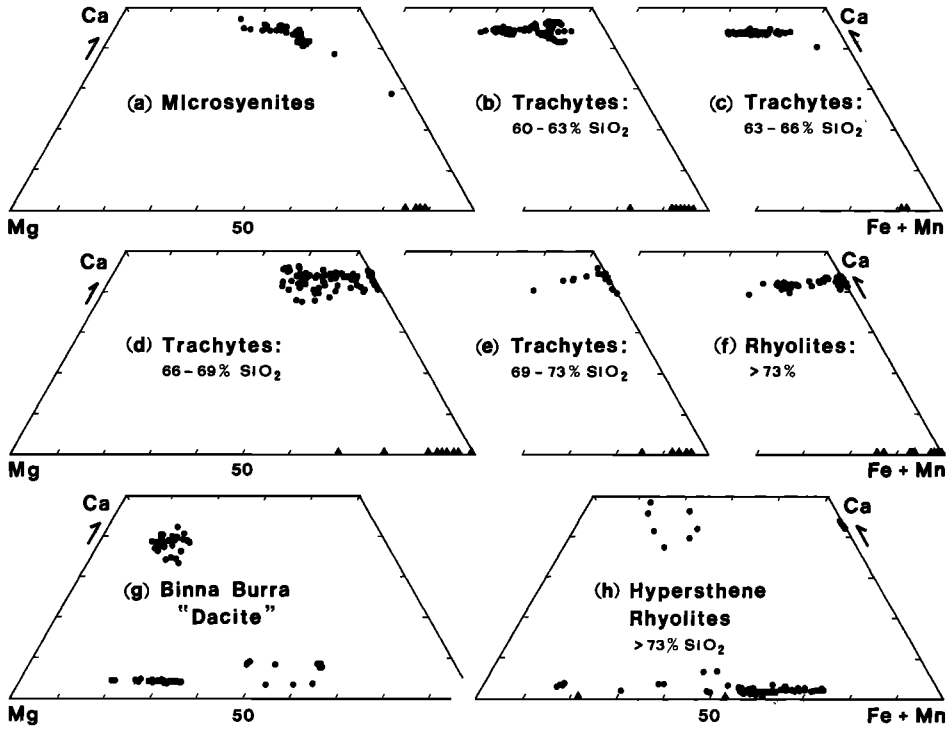

Fig. 8. Composite plots of phenocryst pyroxenes (solid dots) and olivines (solid triangles), based on microprobe data, occurring within the microsyenites, trachytes, and various rhyolite types. Trachyte data subdivided according to total rock silica contents. Atomic percent.

$$NaAlSi_3O_8 + \tfrac{1}{4}O_2 + \tfrac{1}{2}Fe_2SiO_4 = \tfrac{1}{2}Al_2O_3 + NaFeSi_2O_6 + 1\tfrac{1}{2}SiO_2$$
albite gas fayalite liquid acmite (pyroxene S.S.) quartz

$$NaAlSi_3O_8 + \tfrac{1}{2}Fe_2O_3 = \tfrac{1}{2}Al_2O_3 + NaFeSi_2O_6 + SiO_2$$
albite hematite (ilmenite S.S.) liquid acmite (pyroxene S.S.) quartz

These reactions can be applied in principle to the nonperalkaline rhyolites of the region (containing alkali feldspar, calcic pyroxenes, ilmenite, quartz, and fayalite), to the microsyenites, and also to the syenites of the Mt. Warning complex [*Ewart et al.*, 1976]; these microsyenites and syenites show late-stage Na-enrichment of the constituent calcic pyroxenes in the presence of quartz, alkali feldspar, ilmenite, and fayalite.

The first reaction suggests that $a_{NaFeSi_2O_6}^{pyroxene}$ is likely to be sensitive to changes of $a_{Al_2O_3}^{liquid}$ and fO_2 (and also $a_{SiO_2}^{liquid}$). This is illustrated in Figure 10*a* (modified from *Ewart et al.*[1976],) assuming $a_{SiO_2}^{quartz} = a_{Fe_2SiO_4}^{olivine} = 1$, and $a_{NaAlSi_3O_8}^{feldspar} = 0.75$, with the calculations repeated for the three stated oxygen buffers. The results suggest that for a given $a_{Al_2O_3}^{liquid}$ and T, increasing fO_2 favors increasing $a_{NaFeSi_2O_6}^{pyroxene}$, whereas if crystallization follows a constant fO_2 buffer, then decreasing $a_{Al_2O_3}^{liquid}$ favors increasing $a_{NaFeSi_2O_6}^{pyroxene}$.

TABLE 2. Selected Averaged Microprobe Analyses of Phenocrystal Ferroaugites and Ferrohedenbergites From Rhyolites and Trachytes

	1	2	3	4	5	6	7	8
SiO_2	50.12	49.37	49.25	48.97	47.30	48.19	47.54	48.28
TiO_2	0.58	0.49	0.54	0.29	0.38	0.43	0.30	0.32
Al_2O_3	1.13	1.15	0.85	0.49	0.63	0.90	0.83	0.24
Fe_2O_3*	1.33	1.17	1.46	0.57	0.25	—	2.50	0.92
FeO*	19.27	20.37	22.13	25.50	30.93	30.25	28.17	30.12
MnO	0.69	0.71	0.81	0.66	0.78	0.75	1.11	0.81
MgO	6.90	5.87	4.84	4.12	0.21	0.20	0.03	0.03
CaO	20.26	19.91	19.99	18.63	18.46	19.43	19.35	18.04
Na_2O	0.48	0.52	0.47	0.29	0.25	0.38	0.64	0.84
Σ	100.75	99.56	100.35	99.61	99.19	100.53	100.47	99.60

1, 3—Fraser Island trachytes (samples 36367 and 38986); 2—Glass Houses trachyte (sample 38669)†; 4, 5—Mt. Gillies rhyolites (33030, 9570); 6—Mt. Flinders trachyte (38702); 7—Minerva Hills trachyte (38739c); 8—Mt. Alford rhyolite (38710c).

* Calculated on basis of O = 6; cations = 4.

† Sample numbers listed in Tables 2–8 refer to collections in Department of Geology, University of Queensland.

TABLE 3. Selected Averaged Microprobe Analyses of Phenocrystal Orthopyroxenes (1–3) and Ferropigeonite (4) From Rhyolites

	1	2	3	4
SiO_2	48.30	48.12	49.39	49.95
TiO_2	0.23	0.19	0.53	0.55
Al_2O_3	0.94	0.36	0.89	0.74
Fe_2O_3*	2.46	0.38	—	2.11
FeO*	34.18	40.64	35.28	26.87
MnO	0.69	0.80	0.75	0.72
MgO	12.08	8.37	12.57	15.50
CaO	0.71	0.91	0.54	3.03
Na_2O	0.14	0.14	0.04	0.24
Σ	99.73	99.81	99.99	99.71

1—Springbrook rhyolite (sample 31052); 2—Mt. Alford rhyolite (38990); 3, 4—Mt. Gillies rhyolites (samples 33033, 33037).
* Calculated on basis of O = 6; cations = 4.

Figure 10*b* illustrates the relationship between $a_{Al_2O_3}^{liquid}$ and $a_{NaFeSi_2O_6}^{pyroxene}$ as calculated from the second reaction and utilizing estimates of $a_{Al_2O_3}^{liquid}$ for the comendites and the Mt. Gillies metaluminous rhyolites from the reactions and data listed in *Ewart et al.* [1976]. It is further assumed that $a_{Fe_2O_3}^{ilmenite} = 0.03$, with the activities of the other components as above. The relatively higher $a_{NaFeSi_2O_6}^{pyroxene}$ calculated for the comenditic pyroxenes is thus consistent with observation, although it should be noted that reaction (2) is not strictly applicable to those comendites not containing ilmenite.

In summary, the reactions considered suggest that the progressive development of decreasing $a_{Al_2O_3}^{liquid}$ during the petrogenesis of certain groups of the southern Queensland silicic magmas will result in pyroxene Na-enrichment; this presumably must represent an advanced stage of fractionation of these magmas. The stage at which Na-enrichment actually occurs, however, is likely to be controlled by additional parameters such as fo_2 and $a_{SiO_2}^{liquid}$ (i.e., is dependent on the mineral assemblages present). In these Queensland silicic magmas it will be subsequently shown that crystallization occured at an fo_2 below the QFM buffer, which is evidently consistent with the development of pyroxene Na-enrichment only in extreme Fe-enriched pyroxene compositions.

Olivines. Compositions range from approximately Fa_{70} to pure fayalite, most analyzed compositions being between Fa_{90} and Fa_{100}. Olivines occur throughout the trachyte-rhyolite compositional range only as phenocryst phases, but are very rare in comendites.

Amphiboles and Biotites

Three distinct occurrences of amphibole (Figure 11 and Table 5) can be recognized as follows, using the nomenclature of *Ernst* [1968]: (a) pure Fe-hastingsite, occurring as phenocrysts only in certain of the Minerva Hills trachytes. This amphibole shows little chemical variation. A typical formula is $(Ca_{1.77}Na_{0.73}K_{0.34})$ $(Fe_{4.56}Mn_{0.10}Ti_{0.34}Al_{0.10})$ $(Al_{1.63}Si_{6.37})$ $(OH_{1.71}F_{0.29})$; (b) fluorarfvedsonite, characteristic as a groundmass phase within the peralkaline extrusives. They are strongly Mg depleted and contain significant ZrO_2; (c) intermediate Na-Ca amphiboles, classified as ferrorichterites, oc-

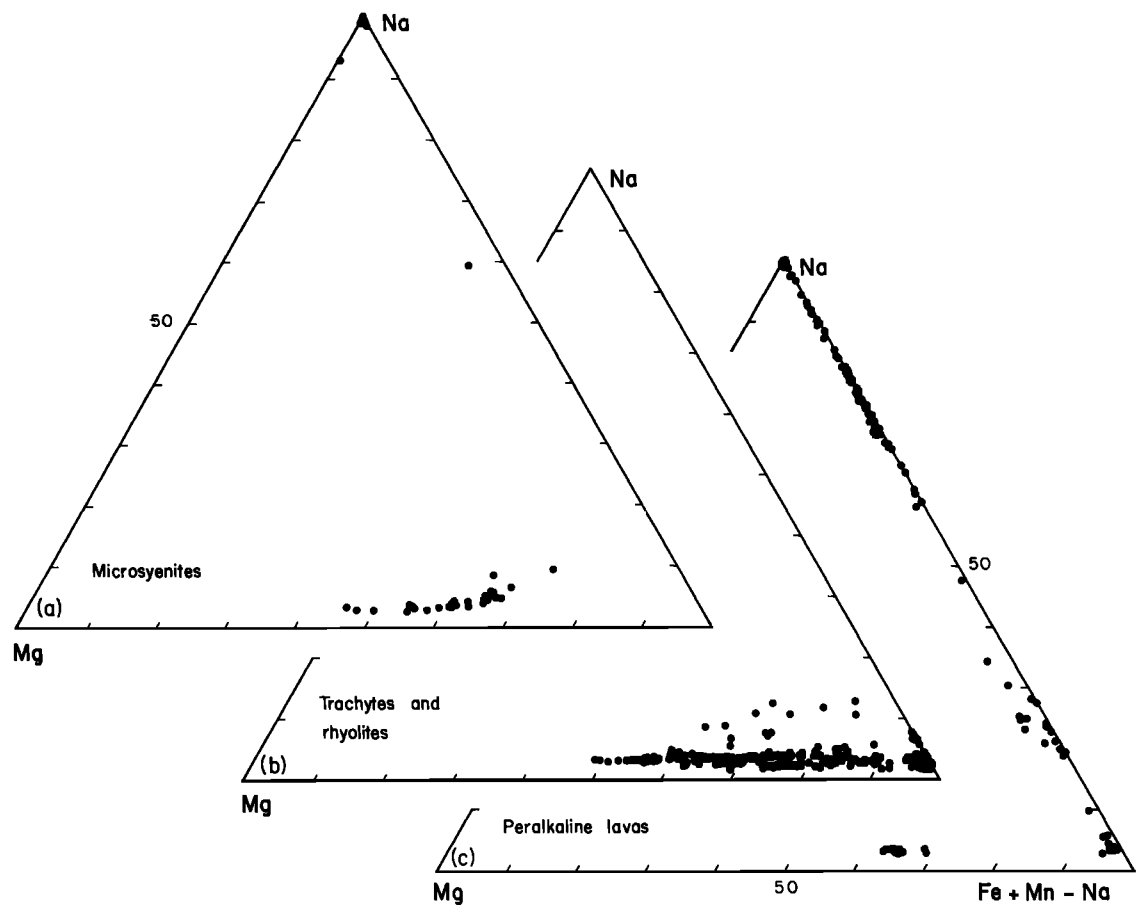

Fig. 9. Composite plots, based on microprobe data, comparing the levels of Na enrichment within the pyroxenes occurring within the microsyenites, trachytes and rhyolites, and peralkaline extrusivs. Atomic percent.

TABLE 4. Selected Averaged Microprobe Analyses of Groundmass Sodic Pyroxenes From Peralkaline Trachytes and Comendites

	1	2	3	4	5	6	7
SiO_2	51.59	50.80	52.04	52.80	51.58	48.64	51.76
TiO_2	1.43	0.81	3.58	1.16	0.45	0.21	1.18
ZrO_2	2.92	2.85	0.56	0.77	2.43	0.49	0.18
Al_2O_3	0.23	0.17	0.22	0.47	1.01	0.68	0.34
Fe_2O_3*	22.43	18.50	25.87	29.01	24.28	8.52	29.79
FeO*	6.45	11.04	3.87	1.72	5.79	20.03	1.89
MnO	0.36	0.63	0.35	0.15	0.26	1.01	0.55
MgO	—	0.01	—	—	0.03	0.54	0.06
CaO	2.61	5.35	0.43	0.93	2.61	16.54	1.54
Na_2O	11.69	9.56	13.08	13.20	11.59	3.31	12.55
Σ	99.71	99.72	99.99	100.22	100.02	99.96	99.85

1, 2—Glass House Mountains comendite and trachyte (38672, 38605); 3—Binna Burra comendite (15779); 4—Mt. Alford comendite (538); 5, 6—Warrumbungle Mountains trachyte (38993), aegirine and aegirine augite; 7—Nandewar Mountains trachyte (39000).

* Calculated on basis of O = 6; cations = 4.

curring as interstitial phases within the intrusive microsyenites. These amphiboles are more magnesian than the above-described amphiboles, in conformity with the associated more magnesian pyroxenes in the microsyenites.

Biotite is a very rare phenocryst phase in the silicic magmas, occurring in certain rhyolites (Figure 12; Table 5). The compositions are again very Fe-rich and approach annite. F is present, but has probably been reduced by posteruption hydroxyl exchange. Coexisting Fe-Ti oxides are absent in these biotite-bearing rhyolites.

Fe-Ti Oxides

Nonperalkaline eruptives. Within the lower SiO_2 trachytes (<66%), titanomagnetite (ulvöspinel 40–75 mol. %) is the sole oxide phase (including phenocrysts and groundmass). Coexisting, discrete phenocryst titanomagnetite and ilmenite do occur in some, but by no means all, of the more siliceous trachytes; only in the vitreous or extremely fine-grained lavas are the oxides homogeneous. These spinel phases are characterized chemically (Table 6) by very low Mg, V, and Cr levels, and variable Mn.

Within the rhyolites, there is an almost complete absence of a phenocryst spinel phase; the only oxide phase is normally an almost stoichiometric phenocryst ilmenite (Table 7). One exception is found in a single Binna Burra rhyolite flow that contains trace quantities of almost pure ulvöspinel (Usp. 95–99 mol. %; see *Ewart et al.* [1977]).

Peralkaline eruptives. Fe-Ti oxides are commonly absent,

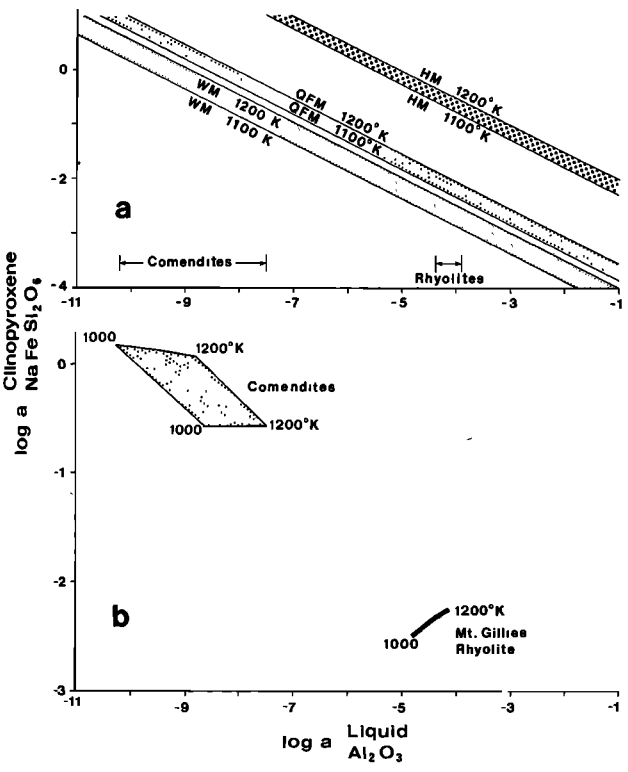

Fig. 10. Schematic plots illustrating the calculated relationships between $a_{NaFeSi_2O_6}^{clinopyroxene}$ and $a_{Al_2O_3}^{liquid}$, utilizing reactions (l) (Figure 10*a*) and (s) (Figure 10*b*) given in the text. In Figure 10*a* the data are plotted for the three fo_2 buffers, each calculated at 1 bar for two temperatures (1100° and 1200°K). Based on thermodynamic data from *Stull and Prophet* [1971], *Nicholls and Carmichael* [1969], *Marsh* [1975], and *Robie et al.* [1978]. Estimates of $a_{Al_2O_3}^{liquid}$ for the rhyolitic and comenditic magmas is based on reactions given in *Ewart et al.* [1976]. See text for further details.

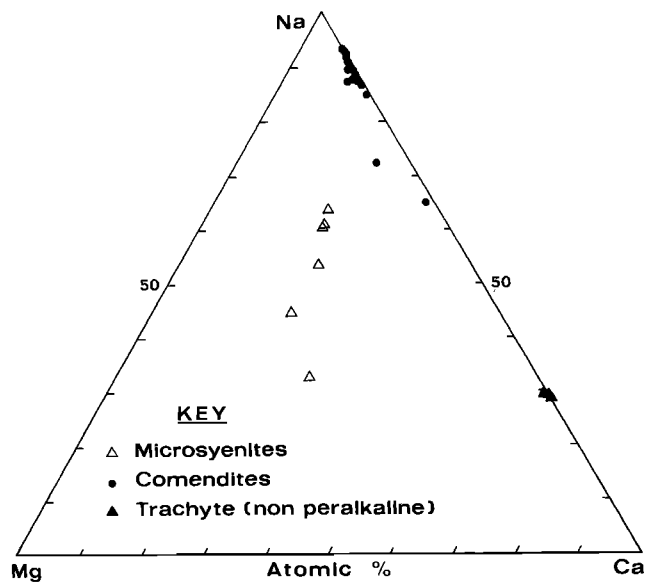

Fig. 11. Plot of amphibole compositions, in terms of Mg, Na, and Ca (atomic %), from microsyenites, trachytes, and comendites. Microprobe data.

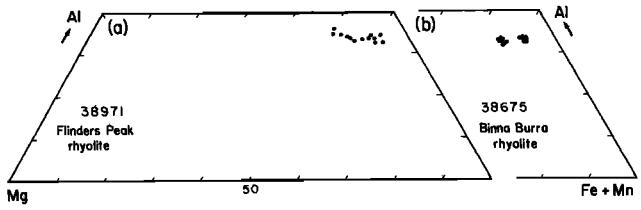

Fig. 12. Compositions of phenocryst biotites, expressed in terms of Al, Mg, and Fe + Mn (atomic %), from two rhyolites. Microprobe data.

but where present they are most frequently represented by ilmenite in the comendites, or less commonly a titanomagnetite in the peralkaline trachytes. In two comendites, disequilibrium-coexisting Fe-Ti oxide phases have been observed. The oxides in the peralkaline magmas are highly depleted in Mg but may contain significant Zn concentrations (Table 7).

$T°C - fo_2$ data. Only relatively few estimates have been made on account of the paucity of suitable coexisting Fe-Ti oxide phases. Available data (using the *Buddington and Lindsley* [1964] geothermometer) are plotted in Figure 13, no data being available for the peralkaline magmas. Equilibration temperatures, for which specific estimates have been determined, lie between 885° and 980°C, with a single microsyenite giving 840°C. All data plot between the QFM and WM buffer curves. It has been previously argued [*Ewart et al.*, 1976] that the presence within the rhyolites of almost stoichiometric ilmenite without a coexisting spinel phase indicates their equilibration at an fo_2 close to the WM buffer, and analogy was drawn with the Skaergaard intrusion [Lindsley et al. 1969]. Thus, these Queensland silicic magmas are interpreted to be relatively reduced, which is consistent with the occurrence of very Fe-enriched ferromagnesian phenocryst silicate assemblages.

Trace Microphenocryst Phases

Chevkinite. This rare-earth titanosilicate is restricted to the ferrohedenbergite-fayalite rhyolites in which it occurs as nonmetamict, euhedral, deep-brown, prismatic microphenocrysts; it may occur as discrete crystals or as inclusions within pyroxene. Modal abundances are estimated to be ≤0.001%. Identification as chevkinite has been confirmed by X ray diffraction, as discussed by *Izett and Wilcox* [1968]. These authors also describe the occurrence of chevkinite in various Cenozoic ash deposits in the western United States. Partial microprobe analyses are presented in Table 8 of two chevkinites occurring in Mt. Gillies and Mt. Alford rhyolite samples. The most notable feature is the huge enrichment in LREE together with significant concentrations of Th, Zr, Nb, and Zn. The compositions are generally similar to those summarized by *Vlasov* [1966].

Allanite. This rare-earth calcium aluminosilicate occurs as discrete, nonmetamict, euhedral, stubby prismatic to equant microphenocrysts. It is found only in those relatively rare rhyolites and trachytes of the region containing Fe-biotite or hastingsitic amphibole. Three of these amphibole-allanite-bearing trachytes give Fe-Ti oxide equilibration temperatures of 920°–980°C, which are significantly higher than the upper limit of 763°C reported for allanite occurrence in the Bishop Tuff by *Hildreth* [1979]. Partial microprobe analyses of selected allanites are presented in Table 8 and are closely comparable to those presented by *Hildreth* [1979]. They exhibit extreme LREE enrichment, with significant Th contents.

Zircon. Euhedral prismatic microphenocrysts of zircon are ubiquitous in the nonperalkaline trachytes and rhyolites but, as previously discussed, are conspicuously absent from the peralkaline lavas. Microprobe analyses of selected zircons (Table 8) indicate HREE enrichment (based on Y data), significant Fe, and Zr/Hf ratios that most commonly range between 41 and 48 but decrease to 26 in zircon from the Binna Burra rhyolite. These Zr/Hf ratios correlate with the available data for the whole rocks, which range from 34 to 45 for most rhyolites, 44 to 50 for the comendites, but decrease to 24 in the most highly fractionated Binna Burra rhyolite.

PETROGENESIS

The anorogenic volcanic suite described is strongly bimodal. *Ewart et al.* [1980] have discussed the possible development of the mafic magmas, concluding that although originally mantle derived, these have undergone lower-crust fractionation within the region of the crust-mantle boundary.

TABLE 5. Selected Averaged Microprobe Analyses of Biotites (1, 2), Calcic Amphiboles (3–5), and Groundmass Arfvedsonites (6–11)

	1	2	3	4	5	6	7	8	9	10	11
SiO_2	34.63	34.13	38.43	38.58	49.32	49.25	49.45	49.30	49.15	48.34	48.41
TiO_2	5.64	4.77	2.65	2.76	2.27	0.58	0.60	0.85	1.08	0.90	1.28
ZrO_2	—	—	—	—	—	1.33	0.78	0.56	0.32	0.77	0.55
Al_2O_3	12.59	12.68	8.39	8.94	0.63	0.66	0.47	0.53	0.38	0.47	0.73
FeO*	29.98	32.69	33.33	33.00	28.61	34.00	34.15	34.27	34.05	33.28	33.25
MnO	0.22	0.17	0.68	0.65	0.55	1.19	0.81	1.16	0.68	1.68	0.89
MgO	2.90	2.01	—	0.05	3.65	0.05	0.06	0.09	—	0.15	0.66
CaO	—	—	9.69	10.02	4.68	2.38	1.55	2.00	1.18	1.81	3.76
Na_2O	0.45	0.46	2.16	2.27	6.21	7.59	7.90	7.86	8.14	7.97	6.70
K_2O	8.51	8.55	1.48	1.63	1.27	1.35	1.38	1.26	1.35	1.17	1.27
F	0.30	0.77	0.49	0.53	n.d.	2.17	2.32	2.44	2.62	2.78	n.d.
Σ†	95.09	95.91	97.09	98.21	97.19	99.64	98.49	99.29	97.85	98.15	97.50

1—Flinders Peak rhyolite (sample 38971), phenocrysts; 2—Binna Burra rhyolite (38675), phenocrysts; 3, 4—Hastingsite, Minerva Hills trachytes (samples 38739a and b), phenocrysts; 5—Ferrorichterite, microsyenite (38979), interstitial phase; 6, 7, 8—Glass Houses comendites (samples 38672, 38606, 38605); 9—Binna Burra comendite (15779); 10—Warrumbungle Mountains peralkaline trachyte (38994); 11—Nandewar Mountains peralkaline trachyte (39000).

* Total Fe as FeO.

† Less 0 for F; n.d., no data.

TABLE 6. Selected Averaged Microprobe Analyses of Titanomagnetite Phenocryst Phases Occurring in Trachytes and Rhyolites

	1	2	3	4	5	6	7
SiO_2	0.09	0.09	0.13	0.27	0.07	0.21	0.07
TiO_2	19.24	20.91	21.13	21.44	22.95	22.60	22.11
Al_2O_3	0.58	0.07	0.16	0.94	0.98	1.28	0.72
V_2O_3	—	—	—	—	0.04	—	0.17
Cr_2O_3	0.01	0.01	—	—	0.02	0.04	0.05
Fe_2O_3*	31.32	28.31	27.03	24.31	23.96	22.34	25.23
FeO*	48.12	48.10	49.69	50.01	51.77	50.91	50.94
MnO	0.66	0.63	0.86	0.72	0.62	1.13	0.45
MgO	0.12	—	0.02	0.04	0.12	—	0.14
CaO	—	—	—	—	—	0.06	—
ZnO	0.37	2.13	n.d.	—	0.38	n.d.	0.30
NiO	—	—	—	—	—	—	—
Σ	100.51	100.26	99.02	97.74	100.91	98.57	100.18
Mol.% Usp	54.6	59.7	61.0	62.8	64.3	65.2	62.5

1, 2—Glass Houses trachytes (38669, 38668); 3—Fraser Island trachyte (38986); 4, 5—Flinders Peak trachytes (38702, 28678); 6—Minerva Hills trachyte (38739a); 7—Mt. Gillies rhyolite (33030).
* Calculated on ulvospinel basis; n.d., no data.

A number of possible paths of evolution may thus be appropriate for the silicic magmas. These include: (a) fractional crystallization from parental basalts; (b) as previously, but with subsequent modification by crustal assimilation/equilibration either during or after fractionation; (c) crustal melting with or without subsequent crystal fractionation. The problem is complicated by the presence of peralkaline and nonperalkaline eruptives in the region, often occurring within the same eruptive center.

The following lines of evidence are relevant to these alternatives:

(a) Within those eruptive centers containing silicic and mafic lavas, the silicic eruptives are always subordinate in volume by at least a 1:7 proportion.

(b) Trace element abundance patterns provide convincing evidence for fractional crystallization control of the rhyolite and comendite chemistries especially. Examples are the extreme depletions of Sr, Ba, V, Mg, P, Cr, and Eu together with the variable enrichment of Rb, U, Th, Nb, Y, and Zn, etc. The trachytes exhibit these trace element patterns to lesser degrees, favoring an interpretation that they represent erupted magmas at progressively less advanced stages of the fractionation processes. Nevertheless, discontinuities in the trace element abundances do occur between the silicic and the exposed mafic lavas.

(c) Normative compositions of the trachytes and rhyolites plot close to the two-feldspar boundary curve and the quartz-feldspar 'minima' in the $(Ab\text{-}Or\text{-}Q)_{97}An_3$ phase system, which again is consistent with crystal-liquid fractionation.

(d) The continuity of phenocryst compositions through the trachyte-rhyolite compositions, especially notable within the pyroxenes and olivines that extend to the pure Fe end-members. An analogy can be drawn here, for example, with the late stages of fractionation of the Skaergaard intrusion [*Brown and Vincent*, 1963].

(e) Fe-Ti oxide equilibration temperatures of the trachytes and rhyolites range from 885° to 980°C. Application of the olivine-clinopyroxene geothermometer [*Powell and Powell*, 1974] suggests temperatures (1 bar) of 890°–1100°C, averaging 976°C for the trachytes and 942°C for the rhyolites. These increase to 920–1130°C if 5 kbar is assumed. Finally, *Ewart et al.* [1976] estimated equilibration temperatures of approximately 900°–1000°C for the Springbrook hypersthene rhyolites, based on calculations of the ilmenite-orthopyroxene exchange reaction. Although varying in their likely reliability, all three temperature estimates are consistent in indicating rel-

TABLE 7. Selected Averaged Microprobe Analyses of Ilmenite Phenocryst Phases Occurring in Trachytes, Rhyolites, and Comendites

	1	2	3	4	5	6	7	8	9	10
SiO_2	—	—	—	—	0.12	—	—	—	—	—
TiO_2	50.23	50.47	48.69	48.24	51.18	51.54	51.44	50.96	50.52	51.57
Al_2O_3	0.02	0.06	0.03	0.08	—	0.06	0.09	0.04	0.04	0.03
V_2O_3	—	—	—	—	—	0.02	0.27	—	—	—
Cr_2O_3	—	—	0.05	—	—	0.01	0.04	—	—	—
Fe_2O_3*	5.00	4.62	6.61	6.09	2.20	0.83	2.39	2.59	3.53	1.38
FeO*	43.86	44.17	42.11	31.29	45.19	45.19	43.24	44.95	43.24	44.39
MnO	1.14	0.73	1.59	11.90	0.96	0.73	0.48	0.72	1.06	1.14
MgO	—	0.22	—	—	—	0.17	1.39	0.01	—	—
ZnO	0.17	0.09	n.d.	n.d.	n.d.	0.13	0.06	0.15	1.27	0.94
NiO	—	—	—	—	—	—	—	—	—	—
Σ	100.42	100.36	99.08	97.60	99.65	98.68	99.40	99.42	99.65	99.45
Mol.%R_2O_3	4.8	4.5	6.5	6.1	2.1	0.9	2.7	2.5	3.4	1.4

1—Glass Houses trachyte (38668); 2—Flinders Peak trachyte (38678); 3, 4—Minerva Hills trachytes (38739a; 38739b, single grain); 5—Mt. Alford rhyolite (38710c); 6—Binna Burra rhyolite (38675); 7—Springbrook rhyolite (38679); 8—Mt. Gillies rhyolite (9570); 9—Glass Houses comendite (38606); 10—Binna Burra comendite (15779).
* Calculated on R_2O_3 basis; n.d., no data.

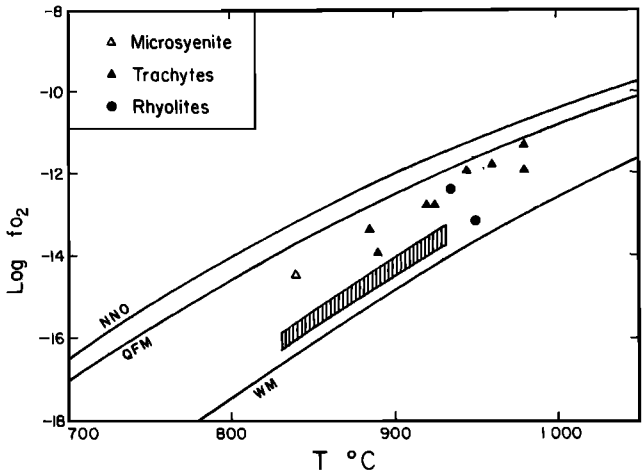

Fig. 13. T(°C)-fo_2 data deduced from coexisting Fe-Ti oxides [*Buddington and Lindsley*, 1964], from a microsyenite, trachytes, and rhyolites. The hatched area is the possible region of equlibration of a single Binna Burra rhyolite sample, in which the Fe-Ti oxides do not give a unique solution [*Ewart et al.*, 1977]. Three buffer curves are plotted (1 bar), representing quartz-fayalite-magnetite, nickel-nickel oxide, and wüstite- magnetite [after *Eugster and Wones*, 1962; *Hewitt*, 1978].

atively high temperatures of phenocryst equilibration, further implying that the magmas were strongly water undersaturated during phenocryst equilibration. This is again consistent with the general paucity of pyroclastics, the paucity of hydrous phenocryst phases, the relatively reducing fo_2 buffer conditions estimated to have existed during phenocryst equilibration, and the occurrence of extremely Fe-enriched phenocryst compositions.

Application of least squares linear mixing calculations [*Bryan et al.*, 1969] have been undertaken to test possible combinations of parental magmas plus mineral compositions and assemblages that can in principle account for the production of specific silicic magma compositions by crystal fractionation. Theoretically, it has been found feasible to derive the comendites, trachytes, and rhyolites from various silica-saturated and undersaturated hawaiite magma compositions from the region [e.g., *Ross*, 1977; *Ewart et al.*, 1977]. The mineral assemblages normally required are plagioclase + olivine + aluminous augite + apatite ± titanomagnetite ± ilmenite ± alkali feldspar. Calculated weight fractions of derivative rhyolitic or comenditic liquids range between 0.05 and 0.18, with plagioclase being the most important subtracted mineral phase (amounting to between 0.4 and 0.5 weight fraction), except where alkali feldspar is also involved. Little difference is noted in these calculations as to the proportions or types of minerals that can produce the peralkaline or nonperalkaline derivatives, with the notable exception of those solutions involving alkali feldspar. This mineral phase always comprises a proportionately higher weight fraction in the feasible solutions involving the peralkaline derivatives. Trace element data do not, however, fully support these least squares mixing calculations. For example, considering the Binna Burra rhyolites, which exhibit the most extreme trace element fractionation abundance patterns in the region, it is possible to readily account for the almost complete Sr depletion (caused by the high weight fractions of feldspar required in the calculated solutions), but it is not possible using the same (or even similar) least squares solutions, to simulate the complementary level of Ba depletion nor the observed high levels of Rb or Pb concentrations. Similar results are obtained for the more fractionated comendites, although the calculations do reproduce the high Zr concentrations. Clearly, therefore, the least squares mixing calculations are not wholly duplicating the inferred crystal fractionation processes, and the trace element data may be indicating the occurrence of additional fractionation phenomena, such as liquid-state differentiation, as advocated to account for similar trace element behavior in the Bishop Tuff [*Hildreth*, 1979]. This is, perhaps, emphasized further by the observed Eu depletion in the Binna Burra rhyolites, which

TABLE 8. Selected Averaged Microprobe Analyses of Microphenocrystal Zircon (1–5), Chevkinite (6–7), and Allanite (8–10), Occurring in Trachytes and Rhyolites

	1	2	3	4	5	6	7	8	9	10
SiO_2	32.44	32.59	31.61	32.38	32.44	19.28	18.41	30.40	30.25	30.54
TiO_2	0.16	0.05	0.05	0.12	0.05	19.58	18.63	2.95	1.72	2.41
ThO_2	0.19	0.07	0.11	0.25	0.17	1.04	0.43	0.36	0.84	0.37
ZrO_2	65.5	65.4	65.9	64.2	65.4	0.80	0.44	—	—	0.05
HfO_2	1.33	1.19	1.41	2.19	1.24	n.d.	n.d.	n.d.	n.d.	n.d.
Al_2O_3	—	—	—	—	—	0.68	0.14	11.47	12.88	12.25
La_2O_3	—	0.02	—	0.01	—	12.6	14.3	8.0	5.9	7.5
Ce_2O_3	0.07	0.03	0.02	0.03	—	20.8	22.2	12.2	11.7	12.2
Nd_2O_3	0.03	0.03	0.03	0.04	—	8.2	7.6	4.0	4.9	4.2
Y_2O_3	0.15	0.33	0.50	0.40	0.41	0.56	0.43	0.19	0.55	0.19
Nb_2O_5	—	—	—	—	—	0.73	0.94	0.05	—	0.04
FeO*	0.30	0.26	0.15	0.45	0.64	9.87	11.04	17.35	16.27	16.63
MnO	—	—	—	—	—	0.10	0.15	0.42	0.23	0.21
MgO	—	—	—	—	—	—	—	—	0.19	0.19
CaO	—	—	—	—	—	3.50	2.64	9.37	9.45	10.18
Na_2O	—	—	—	—	—	—	0.03	0.09	0.13	0.13
F	—	—	—	—	—	0.34	0.28	0.25	0.20	0.23
Σ	100.17	99.97	99.78	100.07	100.35	98.08	97.66	97.10	95.21	97.32
Zr/Hf	42.9	48.0	40.6	25.6	46.1	—	—	—	—	—

1, 2—Mt. Gillies rhyolites (33033, 33030); 3—Mt. Alford hypersthene rhyolite (38990); 4—Binna Burra rhyolite (38675); 5—Springbrook rhyolite (31052); 6—Mt. Gillies rhyolite (33033); 7—Mt. Alford fayalite rhyolite (38710c); 8—Minerva Hills trachyte (38739c); 9—Binna Burra rhyolite (38675); 10—Finders Peak rhyolite (38971).

* Total Fe as FeO; n.d., not determined.

based on REE analyses of coexisting feldspars and total rock, is calculated to require at least 95% feldspar fractionation [*Ewart et al.* 1977].

Although the above discussion has dealt with possible fractionation processes in the development of the silicic magmas, the previous data presented cannot be readily used to evaluate crustal contributions caused by equilibration or even fusion processes. The following is a summary tabulation of available isotopic data for the various Queensland magma types [*Ewart et al.*, 1977; and unpublished data, 1981]:

	$\delta O^{18}‰$ (Feldspars)	$(^{87}Sr/^{86}Sr)_0$	$^{206}Pb/^{204}Pb$
Hawaiites, tholeiitic andesites	5.6–7.0	0.7036–0.7046	17.78–18.70
Trachytes	4.9–8.7	0.7043–0.7059	17.78–18.65
Rhyolites	6.9–10.4	0.7071–0.7086	18.40–18,68
Peralkaline lavas	6.2–10.9	0.7048–0.709	17.78–18.57

It is clear that considerable isotopic variability exists within each magma type, but a general increase in $\delta^{18}O$ and initial Sr ratios occurs with increasing silica. Although these isotope data remain to be fully interpreted, the shift of oxygen and Sr compositions certainly suggest the incorporation of some upper crustal components into the magmas either during or after their development [e.g., *Taylor*, 1980]. Moreover, the relatively unradiogenic Pb compositions occurring within certain of the lavas suggests that a moderately old and relatively U-depleted crustal component may also have been at least partially involved.

With respect to the rhyolites, it is still uncertain whether they represent original crustal melts, or are essentially fractionated from parental mafic magma. A possible approach is provided by the Zr experimental results of *Watson* [1979, p. 417], who notes that in magmas whose origins involve crustal partial fusion, their Zr abundances should be buffered at a relatively low and constant level by residual zircon. Thus the relatively lower abundances of Zr in the Binna Burra rhyolites, the hypersthene rhyolites, and to a lesser extent, the Mt. Gillies rhyolites (Table 1), may be indicative of such an origin.

SUMMARY

The following are the currently suggested interpretations of the origins and development of the various silicic extrusive units recognized in the S.E. Queensland-N.E. New South Wales region:

(a) The peralkaline magmas are considered to develop primarily by fractionation, through trachytic derivatives, from parental basaltic or hawaiitic magmas (presumably silica saturated). Isotopic data suggest some crustal equilibration, but to preserve the peralkaline chemistry, little introduction of Al_2O_3 could have occurred (which might be consistent, for example, with a mafic lower crustal wallrock).

(b) The trachytes, including the Minerva Hills trachyte-rhyolite series, are likewise interpreted as derived by fractional crystallization from a parental mafic magma. Isotopic data again indicate a degree of crustal interaction.

(c) The remaining high-silica rhyolites of the region are interpreted to represent local melts generated by partial fusion of relatively dehydrated crustal materials but subsequently modified by fractionation processes of varying intensity.

Viscosity Considerations. Emphasis has been given to the fact that the trace element abundance patterns of the silicic magmas have been controlled by fractionation processes, which are presumed to be dominated by crystal-liquid equilibrium; viscosity considerations, however, suggest some potential difficulties. Using the data of *Shaw* [1972], the viscosities of the average Binna Burra rhyolite and comendite (Table 1) are extrapolated to be approximately 10^{10} and $10^{8.7}$ poises at 900°C, respectively, assuming anhydrous compositions. If 0.5% water is assumed to be present, these values drop to approximately $10^{9.1}$ and $10^{8.3}$, respectively. These viscosities are high, and it seems doubtful as to whether any mechanism of fractionation involving crystal settling could occur (simple calculations indicating, for example, settling rates <1 cm yr^{-1}). One alternative mechanism might be the mechanical segregation of phenocrysts and liquid during flowage through vertical feeder dykes (flowage differentiation; *Komar* [1972, 1976]) caused by the phenomena of grain dispersive pressure, which appears to be favored by increasing fluid viscosity, providing the dyke width is sufficiently small [*Barrière*, 1976]. In principle, this process would seem to allow a more unconstrained degree of crystal-liquid separation than possible in conventional, closed-system crystal settling. Further possibilities, as previously noted, include liquid-state differentiation [*Hildreth*, 1979]. Such additional processes seem to be required by the extreme fractionation exhibited by the trace element abundance patterns within certain groups of the silicic magmas.

Acknowledgments. Most of the analytical work undertaken during this project has been supported by grants from the Australian Research Grants Committee, including support to use the microprobe facility at the University of Melbourne. The generous hospitality of the Department of Geology at the University of Melbourne is gratefully acknowledged. Thanks are also due to A. S. Bagley (University of Queensland) for continued support with X ray analytical work. Thoughtful reviews of the manuscript were provided by W. P. Nash and W. P. Leeman.

REFERENCES

Barrière, M., Flowage differentiation: Limitation of the 'Bagnold Effect' to the narrow intrusions, *Contrib. Mineral. Petrol., 55,* 139–145, 1976

Brown, G. M., and E. A. Vincent, Pyroxenes from the late stages of fractionation of the Skaergaard Intrusion, East Greenland, *J. Petrol., 4,* 175–197, 1963.

Bryan, W. B., L. W. Finger, and F. Chayes, Estimating proportions in petrographic mixing equations by least squares approximations, *Science, 163,* 926–927, 1969.

Buddington, A. F., and D. H. Lindsley, Iron-titanium oxide minerals and synthetic equivalents, *J. Petrol., 5,* 310–357, 1964

Ernst, W. G. Amphiboles, in *Experimental Mineralogy, 1,* Minerals, Rocks, and Inorganic Materials, pp. 1–125, Springer-Verlag, New York, 1968.

Eugster, H. P., and D. R. Wones, Stability relations of the ferruginous biotite, annite, *J. Petrol., 3,* 82–125, 1962.

Ewart, A., A. Mateen, and J. A. Ross, Review of mineralogy and chemistry of Tertiary central volcanic complexes in southeast Queensland and northeast New South Wales, in *Volcanism in Australasia,* edited by R. W. Johnson, pp. 21–39, Elsevier, New York, 1976.

Ewart, A., V. M. Oversby, and A Mateen, Petrology and isotope geochemistry of Tertiary lavas from the northern flank of the Tweed volcano, southeastern Queensland, *J. Petrol., 18,* 73–113, 1977.

Ewart, A., K. Baxter, and J. A. Ross, The petrology and petrogenesis of the Tertiary anorogenic mafic lavas of southern and central Queensland, Australia—Possible implications for crustal thickening, *Contrib. Mineral. Petrol., 75,* 129–152, 1980.

Hewitt, D. A., A redetermination of the fayalite-magnetite-quartz equilibrium between 650°C and 850°C, *Am. J. Sci., 278,* 715–724, 1978.

Hildreth, W., The Bishop Tuff: Evidence for the origin of compositional zonation in silicic magma chambers, *Geol. Soc. Am. Spec. Pap. 180,* 43–75, 1979.

Izett, G. A., and R. E. Wilcox, Perrierite, chevkinite, and allanite in upper Cenozoic ash beds in the western United States, *Am. Mineral., 53,* 1558–1567, 1968.

James, R. S., and D. L. Hamilton, Phase relations in the system $NaAlSi_3O_8$-$KAlSi_3O_8$-$CaAl_2Si_2O_8$-SiO_2 at 1 kilobar water vapour pressure, *Contrib. Mineral. Petrol., 21,* 111–141, 1969.

Komar, P. D., Mechanical interactions of phenocrysts and flow differentiation of igneous dikes and sills, *Geol. Soc. Am. Bull., 83,* 973–988, 1972.

Komar, P. D., Phenocryst interactions and the velocity profile of magma flowing through dikes or sills. *Geol. Soc. Am. Bull., 87,* 1336–1342, 1976.

Lindsley, D. H., G. M. Brown, and I. D. Muir, Conditions of the ferrowollastonite-ferrohedenbergite inversion in the Skaergaard intrusion, East Greenland, in Pyroxenes and Amphiboles: Crystal Chemistry and Phase Petrology, *Mineral. Soc. Am. Spec. Publ., 2,* 193–201, 1969.

Marsh, J. S., Aenigmatite stability in silica-undersaturated rocks, *Contrib. Mineral. Petrol., 50,* 135–144, 1975.

Nicholls, J., and I. S. E. Carmichael, Peralkaline acid liquids: A petrological study, *Contrib. Mineral. Petrol., 20,* 268–294, 1969.

Powell, M., and R. Powell, An olivine-clinopyroxene geothermometer, *Contrib. Mineral. Petrol., 48,* 249–263, 1974.

Robie, R. A., B. S. Hemingway, and J. R. Fisher, Thermodynamic properties of minerals and related substances at 298.15 K and 1 bar (10^5 Pascals) pressure and at higher temperatures, *U.S. Geol. Surv. Bull., 1452,*1–456, 1978.

Ross, J. A., The Tertiary Focal Peak shield volcano, south-east Queensland—A geological study of its eastern flank, Ph.D. thesis, Univ. of Queensland, Brisbane, Australia, 1977.

Shaw, H. R., Viscosities of magmatic silicate liquids: An empirical method of prediction, *Am. J. Sci., 272,* 870–893, 1972.

Stevens, N. C., The petrology of the Mt. Alford ring-complex, S. E. Queensland, *Geol. Mag., 99,* 501–515, 1962.

Stull, P. R., and H. Prophet, JANAF thermochemical tables (2nd ed), *Nat. Stand. Ref. Data Ser., Nat. Bur. Stand. (U.S.), 37,* p. 1141, 1971.

Taylor, H. P., The effects of assimilation of country rocks by magmas on $^{18}O/^{16}O$ and $^{87}Sr/^{86}Sr$ systematics in igneous rocks, *Earth Planet. Sci. Lett., 47,* 243–254, 1980.

Tuttle, O. F. and N. L. Bowen, Origin of granite in the light of experimental studies in the system $NaAlSi_3O_8$-$KAlSi_3O_8$-SiO_2-H_2O, *Geol. Soc. Am. Mem., 74,* 1–153, 1958.

Veevers, J. J., R. G. Mollan, F. Olgers, and A. G. Kirkegaard, The geology of the Emerald 1:250,000 sheet area, Queensland, *Rep. 68,* Bur. Miner. Resour. (Australia), 1964.

Vlasov, K. A. (Ed.), Mineralogy of rare earths, *Geochemistry and Mineralogy of Rare Elements and Genetic Types of Their Deposits,* vol. 2, Academy of Sciences of the USSR, translated from Russian by Z. Lerman, Israel Program for Scientific Translations, Jerusalem, 1966.

Watson, E. B., Zircon saturation in felsic liquids: Experimental results and applications to trace element geochemistry, *Contrib. Mineral. Petrol., 70,* 407–419, 1979.

Wellman, P., and I. McDougall, Cainozoic igneous activity in eastern Australia, *Tectonophysics, 23,* 49–65, 1974.

(Received October 20, 1980;
revised March 19, 1981;
accepted March 25, 1981.)